

RESONANCE OF A ROTARY MACHINE SUPPORT BEAM CONSIDERING GEOMETRIC STIFFNESS

ALEXANDRE M. WAHRHAFTIG

*Federal University of Bahia (UFBA), Polytechnic School, Department of Construction and Structures, Salvador, Brazil
e-mail: alixa@ufba.br*

REYOLANDO M.L.R.F. BRASIL

University of São Paulo (USP), Polytechnic School, Department of Structural and Geotechnical Engineering, São Paulo, Brazil; e-mail: reyolando.brasil@poli.usp.br

THIAGO B. GROBA, LAURO M.L. ROCHA

*Federal University of Bahia (UFBA), Polytechnic School, Department of Construction and Structures, Salvador, Brazil
e-mail: tbgroba@gmail.com; lauromiguel227@gmail.com*

JOSÉ M. BALTHAZAR

*Federal University of Technology of Parana (UTFPR), Department of Electronics, Ponta Grossa, Brazil
e-mail: jmbaltha@rc.unesp.br*

LÁZARO S.M.S.C. NASCIMENTO

*Federal University of Bahia (UFBA), Polytechnic School, Department of Construction and Structures, Salvador, Brazil
e-mail: sabasencivil@hotmail.com*

The effects of axial compressive forces on free vibration frequencies of rotating machine support beams are investigated taking into account their geometric stiffness. One class of structures that has economic and strategic importance is the base of machines, which is excited by vibrations induced by the supported equipment. These vibrations can affect the structures or, more generally, may generate damage to the supported equipment and the quality of production. They may also render human working conditions difficult. In the current work, these effects are studied via mathematical modeling, numerical simulation and experimental evaluation.

Keywords: resonance, geometric stiffness, support of machines

1. Introduction

Dynamic characteristics of structures are known to depend on their stiffness and mass. Based on these two elements, natural frequencies and vibration modes of a system can be determined. However, the initial stiffness of a structure, computed in the unloaded state, can be affected by the presence of loads, and this is called the geometric stiffness. This is the case of compression loads which tend to decrease the stiffness, the vibration frequencies become lower. In the case of tensile forces, one observes the opposite effect. This latter phenomenon is explored in the so-called tensegrity structures, which work as cable-strut assemblies; their stiffness and self-equilibrium states result from interaction of tension in cables and compression in bars, as shown by Ashwear *et al.* (2016). Positive structural effects considering the influence of different pretension schemes were also studied by Zhou *et al.* (2012). Changes in vibratory behavior due to changes in stiffness produced by loading were reported by Chandravanshi and Mukhopadhyay (2017). These authors found that this type of spring experiences a cycle of compressive and tension forces that alter

its stiffness and conditions of operation, interfering with the dynamic response of the supported system.

One type of structures of considerable economic and strategic importance for civil and military industries is the machinery base, which is subject to vibrations induced by the supported equipment. The importance of rotary machines can be measured by intensive research done on the subject in the last years, as reported by Heindel *et al.* (2018). Application of rotors in modern turbomachinery, particularly in the power generation industry, requires continuous diagnosis and control, see Czajkowski *et al.* (2016). Vibration in rotating machinery is a result of dynamic forces caused by moving or unbalanced parts. Machines may vibrate at various frequencies and amplitudes. These vibrations may affect safety of the structure itself, but, in a more general case, they may have detrimental effects on the equipment and quality of the manufactured product. They can also make the working environment of operators difficult. All industrial sectors are subject to these problems, including sensitive fields of oil, wind and atomic energy, marine structures and even high-rise buildings.

Certain cases related to structural engineering can be mentioned as examples of vibration and resonance problems. The latter is defined as the tendency of a mechanical system to display a large-amplitude response when the excitation frequency matches one of the system natural frequencies. This may lead to violent swaying motion and even catastrophic failure. Maximum amplitudes when passing through resonance frequencies are major concerns in the design of machines, see Markert and Seidler (2001). Vibration problems in periodically excited beams were studied by Patel *et al.* (2016), who investigated changes in their linear free vibration frequency ratios. Wang *et al.* (2018) studied the resonance with respect to response analysis for a turbine blade with varying rotating speed where the rotating blade was modeled as a cantilever beam. Analytical and experimental studies of the resonance in beams were also conducted by Ng *et al.* (2002) who numerically studied amplifier factors in a particular internal relation of a system, and by Motallebi *et al.* (2016) who studied jump and bifurcation phenomena in the forced vibration of nonlinear cantilever beams. Within the marine industry, the work of Lin *et al.* (2009) exemplifies a resonance problem for a ship structure and its control. A research by Zou *et al.* (2016) specifically addresses the longitudinal primary resonance response of a marine propulsion shaft. An overview of vibration problems that include resonance aspects affecting motors and their bases, including the Sommerfeld effect, was presented by Balthazar *et al.* (2003). The Sommerfeld effect can be defined as the occurrence of differentiated phenomena when the oscillating system interacts with the source of excitation.

When observing rotary machines in traditional applications, it is possible to verify that the supported equipment is, as a rule, many orders of magnitude more valuable than the supporting structure, both in terms of its cost of acquisition and potential damage. Reduction of quality of production is possible if unacceptable vibrations lead to defects in the manufactured objects. Consider, for example, the supporting structure of an industrial point welding robot for an automotive bodywork. Excessive vibration can lead to imprecision in the welding process, affecting the quality of the vehicle. Although equipment support structures are, in general, oversized, and therefore usually not subject to the effects of geometric stiffness. The tendency of modern structural engineering is towards more slender members, due to the use of more efficient and lightweight materials and increasingly powerful structural analysis tools. In this context, it could be noted that new phenomena and emergent areas were addressed in a recent study by Balthazar *et al.* (2018), concerning structures supporting unbalanced machines capable of only limited power output. The motion of an oscillating structure excited by such energy sources is accompanied by full interaction between these non-ideal motors and their supports.

The model analyzed in the current study is a steel beam supporting an unbalanced rotary machine. It is assumed that the original design took care to keep the natural frequencies of the system away from those of the excitation. The presence of axial compression forces, which

reduce the geometric stiffness of the beam and, consequently, its natural frequencies, can lead to unexpected, potentially dangerous resonance regimes. These effects were analyzed mathematically, numerically and experimentally. First, a mathematical model was developed, and then numerical-computational simulations based on the finite element method (FEM) using academic software were carried out. Finally, a laboratory dynamic tests of physical models to validate our mathematical and numerical models have been performed.

2. Mathematical model

From the mathematical point of view, a beam in flexion constitutes a continuous system with infinite degrees of freedom. A practical way to study motion of a beam is to associate it with a system with a single degree of freedom (SDOF), by recognizing that its deformed axis can be represented mathematically by a certain shape function that reproduces actual displacements, and a generalized coordinate, conveniently chosen to represent their amplitude. Thus, the vibration frequency can be found by equating the maximum deformation energy developed in the motion to the maximum kinetic energy.

Of course, the accuracy obtained by this method depends entirely on the assumed shape function that is chosen to represent the analyzed free vibration mode. The use of a function in this manner was first proposed by Rayleigh (1877), and this approach found a wide range of applications in mechanical vibration problems. The application of the concept of geometric stiffness in engineering practice, as previously discussed, involves a support beam for a rotating machine. Studies of vibration problems that take into consideration geometric stiffness can be found in our previous works, Wahrhaftig (2013-2019).

Consider an unbalanced rotary machine mounted on a beam, subjected to an axial compressive force. It is well known that such forces affect the geometric stiffness and, consequently, the values of undamped free-vibration frequencies. If the structure is designed, as is usually the case, with free vibration frequencies that are far from the machine service angular velocity f_E , the changes in the frequency due to geometric stiffness may lead to the appearance of potentially dangerous resonance conditions. Consider also a simply supported Bernoulli-Euler beam AB , of length L and moment of inertia I , as a support for a motor E_g , made of a linear elastic material with modulus of elasticity E , as shown in Fig. 1. The applied axial compression force P is used to change the geometric stiffness and, consequently, the natural frequencies of vibration $f(P)$ of the structure. The eccentricity between the axis of the motor and the beam is initially ignored.

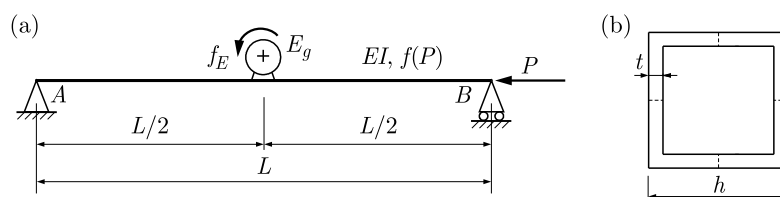


Fig. 1. Beam model: (a) parameters, (b) cross section

The vertical displacement of the midspan point is the generalized coordinate of the system. The undamped vibration frequency in its first mode is obtained using Rayleigh's method.

Consider that the vertical displacement of a generic section of the beam in Fig. 2 is given by

$$v(x, t) = \phi(x)q(t) \quad (2.1)$$

in which $\phi(x)$ is a shape function that satisfies the boundary conditions at the supports and has a unit value at the central section of the beam, whose displacement with time $q(t)$ is our

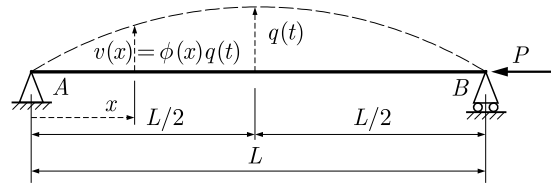


Fig. 2. Analytical model

generalized coordinate. In this case, the shape function given in Eq. (2.2) is adopted, which is the exact solution to the problem without the P load

$$\phi(x) = \sin \frac{\pi x}{L} \quad (2.2)$$

Applying Rayleigh's method, we compute the conventional bending stiffness K_0 associated with the first mode as a function of the material elasticity and the geometry of the cross section as follows

$$K_0 = \int_0^L EI \left(\frac{d^2 \phi(x)}{dx^2} \right)^2 dx = \frac{\pi^4 EI}{2L^3} \quad (2.3)$$

where EI is the flexural bending stiffness, the product of the material modulus of elasticity and the moment of inertia of the section. As a function of the axial force, the geometric stiffness K_G is

$$K_G(P) = P \int_0^L \left(\frac{d\phi(x)}{dx} \right)^2 dx = \frac{P\pi^2}{2L} \quad (2.4)$$

The equivalent generalized mass of the system is

$$M = M_C + M_V \quad (2.5)$$

where M_C is a lumped mass at the midspan and M_V is the generalized mass due to mass of the beam given by

$$M_V = \int_0^L m_V \phi(x)^2 dx = \frac{m_V L}{2} \quad (2.6)$$

in which m_V is mass per unit length. Finally, the frequency of undamped free vibration (in rad/s) is found to be

$$\omega(P) = \sqrt{\frac{K(P)}{M}} \quad (2.7)$$

taking the total beam stiffness as

$$K(P) = K_0 - K_G(P) \quad (2.8)$$

The free undamped frequency of vibration in Hertz of the first mode, taking the sign of the compressive force as positive, is given by

$$f(P) = \frac{\omega(P)}{2\pi} = \frac{1}{2} \sqrt{\frac{\pi^2 EI - PL^2}{L^3(Lm_V + 2M_C)}} \quad (2.9)$$

For numerical evaluation, we consider a simple supported beam with theoretical length L equal to 2 m and a cross-section as defined in Fig. 1b where $t = 1.5$ mm is thickness of the wall and $h = 50$ mm is the external dimension of the square section. It is observed that the presence of the compressive axial force P reduces the beam stiffness and, consequently, its natural frequencies $f(P)$, and this may lead to unexpected, potentially dangerous resonance regimes. This is illustrated in Fig. 3 by the intersection of the solid (beam) and dot (rotating machine) curves. This condition is created by the frequency of the motor $f_E = 13.33$ Hz (800 rpm) and the compressive axial force of 38.25 kN. The natural frequency of the beam is given by Eq. (2.9). It was assumed that the material density is 7850 kg/m³, the lumped mass at the midspan (motor mass) is equal to 4.57 kg, and the material modulus of elasticity is 205 GPa. A numerical simulation considering the creep of concrete can be found in Wahrhaftig *et al.* (2018).

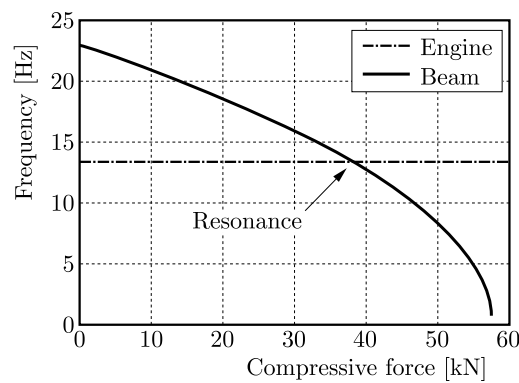


Fig. 3. Structure excitation in the resonant regime

3. Computational modelling

To validate the mathematical models and experimental activity, numerical simulation using FEM was carried out. This is basically an eigenvalues and eigenvectors problem, as given as

$$(\mathbf{K} - \omega^2 \mathbf{M})\Phi = \mathbf{0} \quad (3.1)$$

where \mathbf{M} is the structure mass matrix, and \mathbf{K} is the structure stiffness matrix, which includes the geometric stiffness parcel, in a similar way to Eq. (2.7). In Eq. (3.1), ω^2 are the eigenvalues and Φ are the eigenvectors in the FEM environment. Equation (3.1) is a n -degree polynomial equation, commonly known as the frequency equation. The n solutions for ω_i^2 are real and positive in this case and are squares of the natural frequencies of the system. The known matrices for the mass and stiffness of the six-degree-of-freedom planar beam finite elements are

$$\mathbf{M} = \frac{\rho AL}{420} \begin{bmatrix} 140 & 0 & 0 & 70 & 0 & 0 \\ & 156 & 22L & 0 & 54 & -13L \\ & & 42L^2 & 0 & 13L & -3L^2 \\ & & & 140 & 0 & 0 \\ & symmetric & & & 156 & -22L \\ & & & & & 4L^2 \end{bmatrix} \quad (3.2)$$

and

$$\begin{aligned}
\mathbf{K}_0 = E & \begin{bmatrix} \frac{A}{L} & 0 & 0 & -\frac{A}{L} & 0 & 0 \\ & \frac{12I}{L^3} & \frac{6I}{L^2} & 0 & -\frac{12I}{L^3} & \frac{6I}{L^2} \\ & & \frac{4I}{L} & 0 & -\frac{6I}{L^2} & \frac{2I}{L} \\ & & & \frac{A}{L} & 0 & 0 \\ & \text{symmetric} & & & \frac{12I}{L^3} & -\frac{6I}{L^2} \\ & & & & & \frac{4I}{L} \end{bmatrix} \\
\mathbf{K}_g = \frac{P}{L} & \begin{bmatrix} 0 & 0 & 0 & 0 & 0 & 0 \\ & \frac{6}{5} & \frac{L}{10} & 0 & -\frac{6}{5} & \frac{L}{10} \\ & & \frac{2L^2}{15} & 0 & -\frac{L}{10} & -\frac{L^2}{30} \\ & & & 0 & 0 & 0 \\ & \text{symmetric} & & & \frac{6}{5} & -\frac{L}{10} \\ & & & & & \frac{2L^2}{15} \end{bmatrix}
\end{aligned} \tag{3.3}$$

In Eq. (3.3), the value of the axial force P is computed in the previous static analysis. A single span 3D beam model based on the previously defined geometry was simulated using ANSYS software, academic version 19.0. As this was a 3D model, it was necessary to use a Poisson's coefficient of 0.3. The model has 80 elements, 161 nodes, and 483 degrees of freedom in total. A mesh refinement with the analysis of convergence of results, variations of deformations smaller than 0.01% for finer meshes, and a ratio of the Jacobian equal to one, without distortions, was obtained.

4. Experimental evaluation

To validate the assumed hypothesis, a test bench was designed to perform a physical test, consisting of a steel beam compressed by a hydraulic jack, supporting an unbalanced rotary machine, using the theoretical/numerical approach described previously. When designing the system, the frequency ranges of interest and the horizontal forces to be applied were predicted. The model was then calibrated to the resonance of the first mode of vibration of the structural system.

Figure 4 shows design details of the pinned and roller supports. The former consists of a robust metallic axis with bearings on both sides, placed between short plates located above and below and welded to a square plate fixed at the top of the beam. This prevents any horizontal and vertical motion but allows rotation. Laterally, thick plates were designed to fix this set of parts to the supporting beam by means of pins. The latter is similar to the former, with a bearing of a smaller diameter added to the end of the axis at the point of contact with the support and inserted into a U-shaped profile segment facing vertically inwards. There, a limiter that eliminated the clearance between the bearing and the upper part of the U-shaped bearing was added. Thus, the roller support allows all types of motion in the plane that contains the beam axis, except for vertical motion.

Laterally, on both sides of the beam, U-shaped cold-formed metal profiles served as supports for the central steel beam. Three transverse bracings were arranged along the profiles stiffening

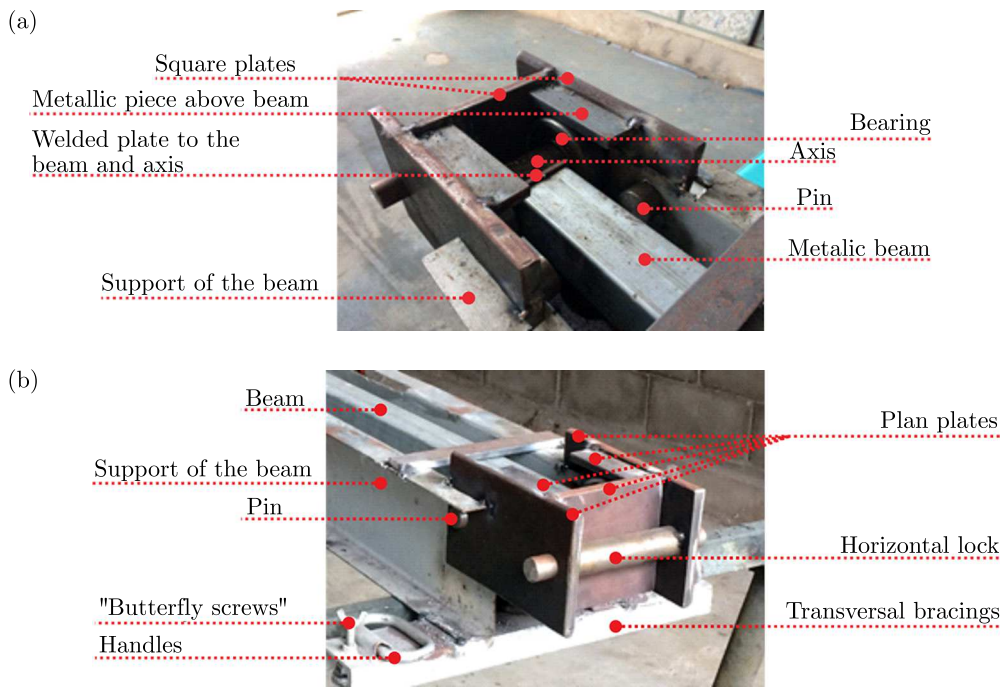


Fig. 4. Pinned (a) and roller support (b)

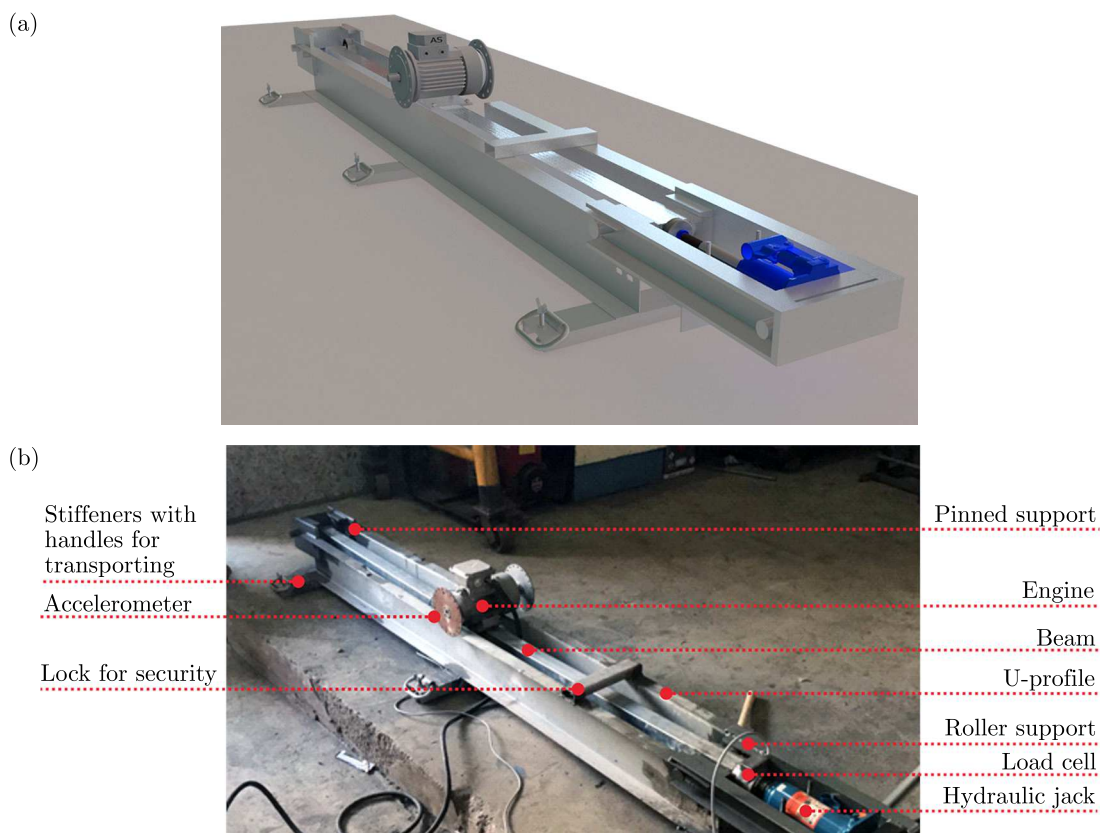


Fig. 5. Test apparatus: (a) 3D image, (b) final prototype

the system in the transverse direction. All of these stiffeners had transport handles and height variators at their extremities. The height variators were butterfly threaded screws with a small circular plate in their extremity, enabling manual adjustment of the verticality of the system. A set of metal parts formed by the union of other U-shaped profiles arranged at the side. The flat plates placed above and below were mounted and joined by welding in order to build the support for the hydraulic jack. This assembly was built before the roller support, outside the theoretical length of the beam.

Figure 5 presents three-dimensional views of the prototype and its service conditions, as on the testing day. The assembly formed in this way was also designed to provide the desired inertial safety for the tests and had at least five times the mass of excitation.

5. Execution

A loading plan based on Eq. (2.9) was prepared in order to force a resonance at the predicted frequencies for each level of the axial compressive force. Once the established force for each stage has been applied, a frequency inverter was used to vary the frequency of the motor from zero to a value little beyond the expected frequency for each axial compressive force level, as shown in Table 1, and then returned it to zero. It is important to mention that the slenderness ratio of the beam was equal to 101, a reasonable value for steel beams.

Table 1. Expected results

Force [kN]	Frequency [Hz]	Force [kN]	Frequency [Hz]
0	22.95	35	14.41
5	21.93	40	12.73
10	20.87	45	10.79
15	19.75	50	8.41
20	18.56	55	5.02
25	17.28	57.76 (Buckling)	0.00
30	15.91		

To compress the beam, a hydraulic jack with a capacity of 80 kN was used. The applied compressive force was varied from zero to 55 kN at intervals of 5 kN. The tests were interrupted when the horizontal force reached approximately 50 kN due to the collapse of the beam. It is possible that the accumulated damage produced by application of the axial compressive force at the previous loading stages contributed to this occurrence, even though all the stresses induced to the beam were below the steel yield stress of 250 MPa, which corresponds to a force of 72.75 kN for the section used. It was assumed that there was no variation in the applied force due to the hydraulic jack, although small oscillations around the set level were observed. It is important to clarify that the jack was a new device, acquired specifically for being used in the experiment and there was no record of any leakage. Interactions of similar nature, such as those present in the supports, losing by friction and damping, and others present in the real system were disregarded. Even so, the physics of the problem was preserved by the adopted model, given by dimension of the parts and forces involved.

The response time histories of structural motions were acquired using a bi-directional accelerometer with a measuring range of $\pm 50g$ (where g is acceleration of gravity). The force was controlled by a 200 kN capacity load cell HBM (2014). Both sensors were connected to a digital data acquisition system and to a laptop computer. Both the accelerometer and the acquisition system, a transportable ADS 1800 with eight channels, were provided by Lynx Electronic Technology (2014). The acquisition rate used for the experiment was 1000 Hz.

6. Results and discussion

A comparison between the mathematical model and FEM simulations is presented in Fig. 6. These simulations agree well with Eq. (2.9) with an average difference between them of less than 1%. All calculations were performed for the undeformed configuration of the beam. Differences smaller than 1.98% were found when considering the longitudinal deformation in the calculation of frequencies. An evaluation of the modal shapes in comparison to the analytical solution given by Eq. (2.2) for different levels of the applied axial loading in the experimental activity was also performed and can be observed for one case due the similarity to the others. There is an average difference of 0.95% in relation to the adopted shape function, considering all the forces acting on it. It was possible to observe that in all cases, the major differences occurred at both extremities of the beam and were smaller towards the middle.

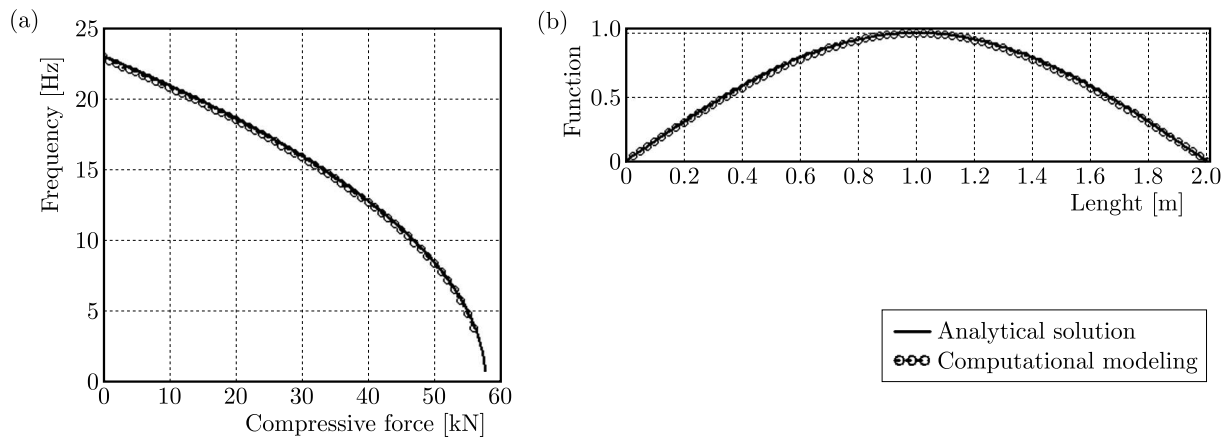


Fig. 6. Analytical and computational results: (a) frequency, (b) modal shape (typical)

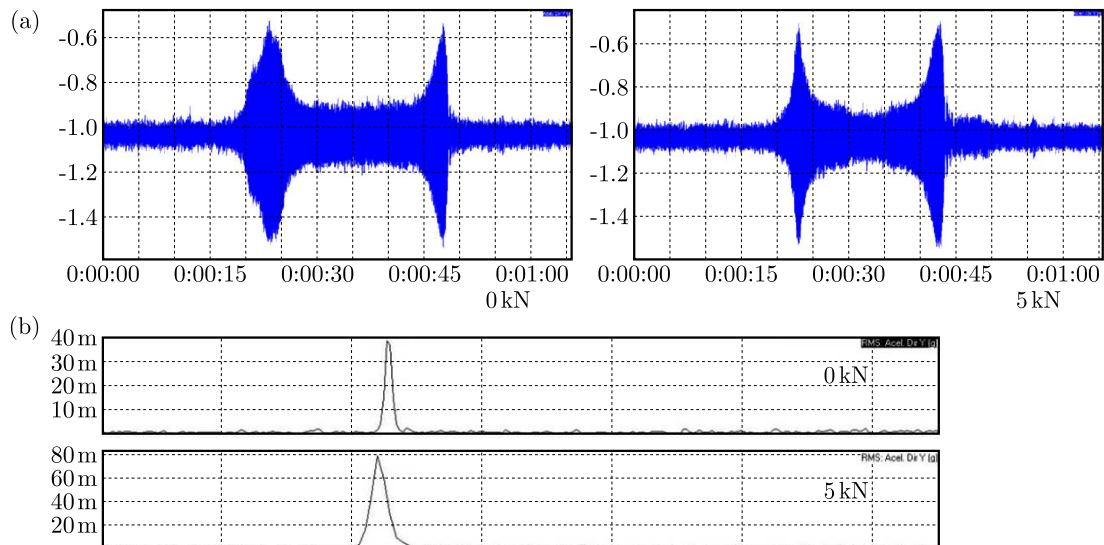


Fig. 7. Representative temporal series (a) and FFT (b) (presented for 0 kN and 5 kN)

The results of the tests are summarized in a temporal series and using the fast Fourier transform (FFT). Figure 7 exemplifies the system resonant frequencies for the levels of axial compressive force of 0 kN and 5 kN. The resonant frequencies were obtained employing the AqDAnalysis Program (Lynx Electronic Technology, 2014) with an interval of time considered appropriate for this study, and using Hanning analysis windows, whose main characteristic is a shape that is similar to a half cycle of a cosine wave.

Based on the results obtained by the FFT analysis, it could be verified that the frequencies remained almost unaltered for changes in the intensity of the applied axial compressive forces (Table 2) contrary to the prediction of the mathematical model. Small variations, which are usual in experimental activity, are observed around the average value of 22.22 Hz (with a standard deviation of 0.89). This experimental evidence led to construction of a new theoretical consideration regarding physics of the problem. A new hypothesis treated the presence of the hydraulic jack as a translational spring, the stiffness of which would cancel out the geometric stiffness parcel.

Table 2. Experimental results obtained

Force [kN]	Frequency [Hz]	Force [kN]	Frequency [Hz]
0	22.71	25	22.71
5	21.97	30	22.46
10	22.46	35	22.95
15	21.48	40	22.46
20	22.95	45	20.02
Average	22.22 Hz		

7. Consideration of a new hypothesis

A new computational model was therefore elaborated to evaluate this hypothesis. This new hypothesis considers that the jack interferes with the vibratory system. This interference is equivalent to the action of a translational spring, as shown in Fig. 8a, where K_s is the spring stiffness coefficient to be experimentally determined. The computational simulation was also adjusted to fit this new hypothesis, and a model including the translational spring can be seen in Fig. 8b. It is useful to mention that springs have been widely applied in the modeling and control of mechanisms of several orders, as affirmed by Fichera and Grossard (2017), and Nie *et al.* (2018).

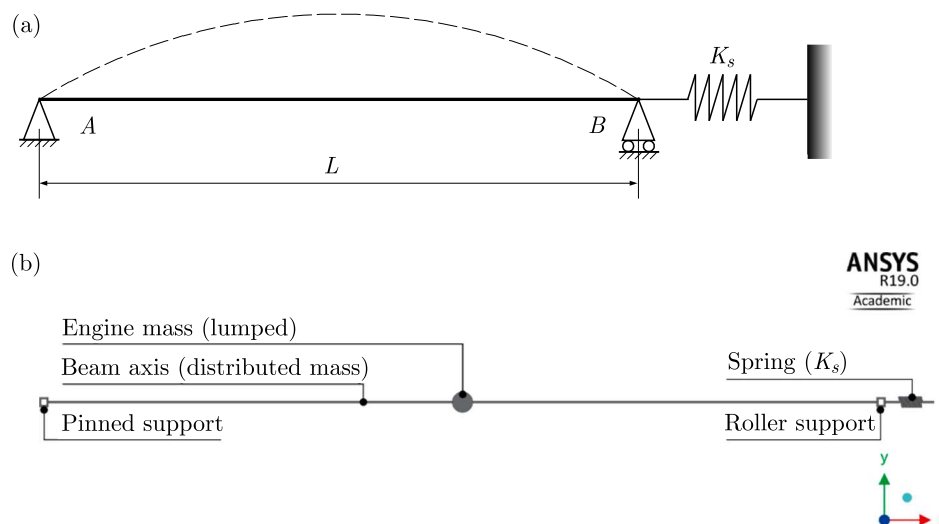


Fig. 8. Adjusted model: (a) analytical and (b) computational

The jack submitted to experimentation was manufactured by Bovenau (2018) and corresponded to a CJ8-8700 model of 80 kN capacity, with a steel cylinder, diameter of 34 mm and length of 147 mm. The hydraulic jack was compressed in a test machine with a 20 mm cylinder

elevation. A value of 83929 kN/m for the spring coefficient was obtained. The results of computational analysis support this adjustment in the mathematical model. That is, frequencies for different levels of the compression force are balanced by the physical presence of the hydraulic jack which acts by introducing a restored force. The results of these new simulations are shown in Table 3. Compared to the experimental results, these frequencies have an average of 21.52 Hz with the average difference of only 2.7%.

Table 3. Results after adjustment of the model

Force [kN]	Computationl [Hz]	Experimental [kN]	Difference [%]
0	22.81	22.71	-0.4
5	22.55	21.97	-2.6
10	22.19	22.46	1.2
15	22.02	21.48	-2.5
20	21.75	22.95	5.2
25	21.48	22.71	5.4
30	21.20	22.46	5.6
35	20.92	22.95	8.8
40	20.64	22.46	8.1
45	20.35	20.02	-1.6
Average	21.59 Hz	22.22 Hz	2.7%

It is important to keep in mind that the frequency of the unloaded beam without the spring, calculated analytically and computationally, was 22.81 Hz, and this value was found to be 22.71 Hz from the experiment, thus coinciding with the unloaded value. Imperfections in terms of construction are therefore of importance in slender beams for these levels of forces. Also it is important to realize the possibility of existing other restoring forces in the system actuating concomitantly to that of the hydraulic jack to keep the experimental frequencies close from the unloaded one.

8. Conclusion

A study of the dynamic behavior of a support beam for a rotating equipment, taking into consideration the effect of axial compression forces acting on its geometric stiffness has been presented. This study was carried out using mathematical models, numerical simulations and laboratory tests of physical scaled models. The basic model elaborated was a metal beam under axial compressive loads, in which variation in the fundamental frequency due to applied forces could lead to resonances that are not predicted by linear theory. The effect on geometric stiffness produced by axial compressive loading and the corresponding possibility of resonant regimes in the structural support system were demonstrated through computation of natural frequencies. In practice, the vibration shapes do not change with the application of such forces.

It was possible to conclude that from the theoretical point of view, resonance conditions can occur due to an increase in the axial compressive force. However, experimental verification of this phenomenon was compromised due to the physical presence of a hydraulic jack, which interfered with observation by behaving as a translational spring, canceling the geometric stiffness and restoring vibratory motions to the axially unloaded state. The mathematical model studied in this paper offers a possible tool for preventing and control unwanted resonance regimes in supporting structures for machines. It can be used as a form of vibration control to avoid harmful effects on the equipment, production process and work environment of the operators. In the further work, experimental investigation that takes into consideration gravitational loads

needs to be conducted as well as further consideration of nonlinear aspects in the presented system.

Funding and acknowledgments

This study was funded by the National Council of Scientific and Technological Development (CNPq) of Brazil (grant “Universal Call MCTI/CNPQ/14/2014, process 443044/2014-7”) and by the São Paulo Research Foundation – FAPESP (Research Grant Process 2017/06076-0). It was supported by the Federal University of Bahia (UFBA) in terms of scholarship. Authors thank to Gabriela Silva Correia Cordeiro for confectioning some images of this work, and Bovenau – Jacks and Hydraulic Equipment – for carrying out the hydraulic jack test.

References

1. ASHWEAR N., TAMADAPU G., ERIKSSON A., 2016, Optimization of modular tensegrity structures for high stiffness and frequency separation requirements, *International Journal of Solids and Structures*, DOI: 10.1016/j.ijsolstr.2015.11.017
2. BALTHAZAR J.M., MOOK D.T., WEBER H.I, BRASIL R.M.L.R.F., FENILI A., BELATO D., FELIX J.L.P., 2003, An overview on non-ideal vibrations, *Meccanica*, DOI: 10.1023/A:1025877308510
3. BALTHAZAR J.M., TUSSET A.M., BRASIL R.M.L.R.F, FELIX J.L.P., ROCHA R.T., JANZEN F.C., NABARRETE A., OLIVEIRA C., 2018, An overview on the appearance of the Sommerfeld effect and saturation phenomenon in non-ideal vibrating systems (NIS) in macro and MEMS scales, *Nonlinear Dynamics*, DOI: 10.1007/s11071-018-4126-0
4. BOVENAU J. AND HYDRAULIC EQUIPMENT, 2018, <http://www.bovenau.com.br/> (in Portuguese), accessed April 2018
5. CHANDRAVANSI M.L., MUKHOPADHYAY A.K., 2017, Analysis of variations in vibration behavior of vibratory feeder due to change in stiffness of helical springs using FEM and EMA methods, *Journal of the Brazilian Society of Mechanical Sciences and Engineering*, DOI: 10.1007/s40430-017-0767-z
6. CZAJKOWSKI M., GERTNER M., CIULKIN M., 2016, Control of anisotropic rotor vibration using fractional order controller, *Journal of Theoretical and Applied Mechanics*, DOI:10.15632/jtam-pl.54.3.1013
7. FICHERA F., GROSSARD M., 2017, On the modeling and identification of stiffness in cable-based mechanical transmissions for robot manipulators, *Mechanism and Machine Theory*, DOI: 10.1016/j.mechmachtheory.2016.10.020
8. HBM – Test and Measurement, 2014, User Guide and Specifications, São Paulo (in Portuguese)
9. HEINDEL S., MÜLLER P.C., RINDERKNECHT S., 2018, Unbalance and resonance elimination with active bearings on general rotors, *Journal of Sound and Vibration*, DOI: 10.1016/j.jsv.2017.07.048
10. LIN T.R., PAN J., O’SHEA P.J., MECHEFSKE C.K., 2009, A study of vibration and vibration control of ship structures, *Marine Structures*, DOI: 10.1016/j.marstruc.2009.06.004
11. Lynx Electronic Technology, 2014, User Guide for AqDados/AqDAnalysis, São Paulo (in Portuguese)
12. MARKERT R., SEIDLER M., 2001, Analytically based estimation of the maximum amplitude during passage through resonance, *International Journal of Solids and Structures*, DOI: 10.1016/S0020-7683(00)00147-5
13. MOTALLEBI A., IRANI S., SAZESH S., 2016, Analysis on jump and bifurcation phenomena in the forced vibration of nonlinear cantilever beam using HBM, *Journal of the Brazilian Society of Mechanical Sciences and Engineering*, **38**, 515-524, DOI: 10.1007/s40430-015-0352-2
14. NG L., RAND R., O’NEIL M., 2002, Slow passage through resonance in Mathieu’s equation, *Journal of Vibration and Control*, DOI: 10.1177/1077546303009006004

15. NIE S., ZHUNG Y., CHEN F., WANG Y., LIU S., 2018, A method to eliminate unsprung adverse effect of in-wheel motor-driven vehicles, *Journal of Low Frequency Noise Vibration and Active Control*, DOI: 10.1177/1461348418767096
16. PATEL B.P., IBRAHIM S.M., NATH Y., 2016, On the internal resonance characteristics of curved beams, *Journal of Vibration and Control*, DOI: 10.1177/1077546314547375
17. RAYLEIGH J.W.S., 1877, *Theory of Sound*, re-issued (1945) Dover Publications, New York
18. WAHRHAFTIG A.M., 20019, Analysis of the first modal shape using two case studies, *International Journal for Computational Methods*, DOI: 10.1142/S0219876218400194
19. WAHRHAFTIG A.M., BRASIL R.M.L.R.F., 2016, Vibration analysis of mobile phone mast system by Rayleigh method, *Applied Mathematical Modelling*, DOI: 10.1016/j.apm.2016.10.020
20. WAHRHAFTIG A.M., BRASIL R.M.L.R.F., 2017, Initial undamped resonant frequency of slender structures considering nonlinear geometric effects: The case of a 60.8 m-high mobile phone mast, *Journal of the Brazilian Society of Mechanical Sciences and Engineering*, DOI: 10.1007/s40430-016-0547-1
21. WAHRHAFTIG A.M., BRASIL R.M.L.R.F., BALTHAZAR J.M., 2013, The first frequency of cantilevered bars with geometric effect: A mathematical and experimental evaluation, *Journal of the Brazilian Society of Mechanical Sciences and Engineering*, DOI: 10.1007/s40430-013-0043-9
22. WAHRHAFTIG A.M., BRASIL R.M.L.R.F., NASCIMENTO L.S.M.S. C., 2018, Analytical and mathematical analysis of the vibration of structural systems considering geometric stiffness and viscoelasticity, numerical simulations in engineering and science, *IntechOpen*, DOI: 10.5772/intechopen.75615
23. WANG D., HAO Z., CHEN Y., ZHANG Y., 2018, Dynamic and resonance response analysis for a turbine blade with varying rotating speed, *Journal of Theoretical and Applied Mechanics*, DOI: 10.15632/jtam-pl.56.1.31
24. ZHOU Z., MENG S.-P., WU J., 2012, A whole process optimal design method for prestressed steel structures considering the influence of different pretension schemes, *Advances in Structural Engineering*, DOI: 10.1260/1369-4332.15.12.2205
25. ZOU D., JIAO C., TA N., RAO Z., 2016, Forced vibrations of a marine propulsion shafting with geometrical nonlinearity (primary and internal resonances), *Mechanism and Machine Theory*, DOI: 10.1016/j.mechmachtheory.2016.07.003